

An MPC Approach to Transient Control of Liquid-Propellant Rocket Engines

Sergio Pérez-Roca ^{*,***} Julien Marzat ^{*} Émilien Flayac ^{*}
Hélène Piet-Lahanier ^{*} Nicolas Langlois ^{**} François Farago ^{***}
Marco Galeotta ^{***} Serge Le Gonidec ^{****}

^{*} DTIS, ONERA, Université Paris-Saclay, Chemin de la Huniere, 91120 Palaiseau, France (e-mails: {sergio.perez_roca, julien.marzat, emilien.flayac, helene.piet-lahanier}@onera.fr)

^{**} Normandie Université, UNIROUEN, ESIGELEC, IRSEEM, Rouen, France (e-mail: nicolas.langlois@esigelec.fr)

^{***} CNES - Direction des Lanceurs, 52 Rue Jacques Hillairet, 75612 Paris, France (e-mails: {francois.farago, marco.galeotta}@cnes.fr)

^{****} ArianeGroup SAS, Forêt de Vernon, 27208 Vernon, France, (e-mail: serge.le-gonidec@ariane.group)

Abstract:

The current context of launchers reusability requires the improvement of control algorithms for their liquid-propellant rocket engines. Their transient phases are generally still performed in open loop. In this paper, it is aimed at enhancing the control performance and robustness during the fully continuous phase of the start-up transient of a generic gas-generator cycle. The main control goals concern end-state tracking in terms of combustion-chamber pressure and chambers mixture ratios, as well as the verification of a set of hard operational constraints. A controller based on a nonlinear preprocessor and on linear MPC (Model-Predictive Control) has been synthesised, making use of nonlinear state-space models of the engine. The former generates the full-state reference to be tracked while the latter achieves the aforementioned goals with sufficient accuracy and verifying constraints for the required pressure levels. Robustness considerations are included in the MPC algorithm via an epigraph formulation of the *minimax* robust optimisation problem, where a finite set of perturbation scenarios is considered.

Keywords: Liquid-propellant rocket engines, model predictive and optimisation-based control, tracking, control of constrained systems, robustness, transients.

1. INTRODUCTION

In the current context of launcher vehicles design, reusability is considered as a major factor. From the automatic control perspective, the potential need for reusable liquid-propellant rocket engines (LPRE) implies stronger robustness requirements than controlling expendable ones due to their multi-restart and thrust-modulation capabilities. The classical multivariable control of main-stage LPRE had attained a reduced throttling envelope (70%-120%) in test benches. At real flights, only the nominal operating point is generally targeted. In the future European *Prometheus* engine, it is aimed at throttling down to 30% (Baiocco P. and Bonnal C. (2016)). Thus, an enlarged validity domain for reusability has to be conceived. At least, it becomes crucial to maintain tracking and robustness at those low throttle levels, where physical phenomena are more difficult to anticipate.

The main control problem in these multivariable systems primarily consists in tracking set-points in combustion-chamber pressure and mixture ratio, whose references stem from launcher needs. Control-valves opening angles are adjusted in order to adapt engine's operating point while respecting some constraints. The most common control

approaches identified in the literature rely on linearised models about operating points for synthesising steady-state controllers, most of them based on PID techniques (such as Nemeth E. et al. (1991)). Generally, initial MIMO (Multi Input Multi Output) systems are considered decoupled into dominant SISO (Single Input Single Output) subsystems. Off-line optimisation strategies have also been carried out (Dai X. and Ray A. (1996)). More complex approaches present in the literature, incorporating some nonlinear (Lorenzo C.F. et al. (2001)), hybrid (Musgrave J.L. et al. (1996)) or robust (Saudemont R. and Le Gonidec S. (2000)) techniques, enhance certain aspects of performance and robustness. And in the event that a component fails, some reconfiguration-control strategies have been proposed (Musgrave J.L. et al. (1996)). To the best of our knowledge, there are no publications which consider not only the steady state but also the demanding transient phases at the same level of performance and robustness, as reviewed in Pérez-Roca S. et al. (2019). Pre-defined sequences of engine operation (start-up and shutdown), are traditionally managed in open loop with narrow correction margins. They consist in an initial succession of discrete events including valves openings and chambers ignitions. Once these commands have all

been executed, the second part of the transient, which is completely continuous, takes place until the steady state is achieved. The main reasons for performing open-loop (OL) control in the first (discrete-event) phase, explained in Nemeth E. et al. (1991), are controllability and observability issues at very low mass flows. Transient control through valves starts to be plausible once all events have finished. This observation has been considered in this paper, where only the second part of the start-up transient, fully continuous, is controlled.

The objective of this work is to control the start-up transient of a pump-fed LPRE. In this case, a gas-generator-cycle engine is targeted. Concretely, it is aimed at achieving combustion-pressure and mixture-ratio end-state tracking while complying with hard operational constraints, mainly concerning mixture ratios, turbopumps rotational speeds and valves actuators angular velocities. The control strategy presented in this paper is based on Model Predictive Control (MPC), which is accompanied by a preprocessor for full-state reference generation. This method was selected as the most appropriate for this kind of complex systems with hard operational constraints, as introduced in the next sections. Indeed, it is more and more used in industry and can be extended for instance with robustness (Mayne D.Q. et al. (2000)) or hybrid considerations, which will be interesting for future work on this topic.

This paper is organised as follows. Section 2 serves as a recapitulation of modelling considerations published in a previous paper. The state-space system used in the following sections is presented there. Section 3 describes the control strategy carried out, which mainly consists in the use of MPC techniques. Section 4 depicts results and includes their analysis. Finally Section 5 serves as a conclusion.

2. MODELLING

The modelling strategy used in this paper was introduced in Pérez-Roca S. et al. (2018). Several types of models are employed in the control loop in this paper. Concerning the plant on which the control is exerted, a simulator of the real plant was constructed in first place. This simulator, whose structure is built component-wise, already considers the basic thermo-fluid-dynamics and mechanics of LPRE elements: mass, energy and momentum conservation equations. The engine considered in this paper, representative of the *Vulcain 1*, presents a gas-generator (GG) cycle. In Fig. 1, its main components are depicted and the main acronyms are summarised. It consists in a *LOX/LH₂* (liquid oxygen as oxidiser, liquid hydrogen as fuel) engine. The hot-gas flow necessary to drive turbines comes from a GG, a small combustion chamber that receives a small portion of the main propellant flow. The actuators considered in this paper are five continuously-controllable valves (VCH, VCO, VGH, VGO and VGC). Apart from those, there are two discrete actuators: one binary igniter (*i_{CC}*) and one binary starter (*i_{GG}*). However, they are considered as active in this paper in order to treat the continuous part of transients (up from 1.5s after start command), where only continuous control takes place. The GG starter injects hot gas into that cavity during less than 1.5s so as to start driving turbines. Valves angles (α), which have a nonlinear but direct relation to sections

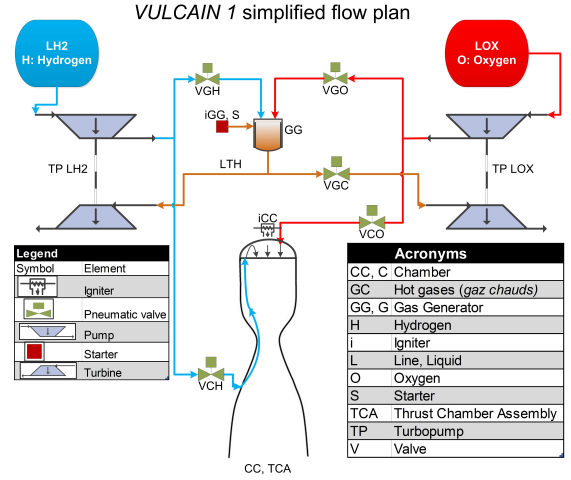


Fig. 1. *Vulcain 1* simplified flow plan

(A), control the flows to the main combustion chamber (VCH and VCO), to the GG (VGH, VGO), and to the oxidiser turbine (VGC). The latter consists in the main contribution in determining mixture ratio (MR), which is defined as the quotient between oxidiser and fuel mass flow rates $MR = \dot{m}_{ox}/\dot{m}_{fu}$. This ratio, a major performance indicator in LPRE, is established at three levels: at an engine's global level (MR_{PI}), taking pumped propellants into account; in the combustion chamber (MR_{CC}) and in the GG (MR_{GG}).

The simulator was then translated into a nonlinear state-space model by joining components equations symbolically. At this stage, having already carried out certain simplifications with respect to the initial simulator, the model is referred to as *complex NLSS* (nonlinear state-space) or $f_c(\mathbf{x}, \mathbf{u})$. However, this model was too cumbersome for control design. Hence, it was further reduced until achieving the here-called *simplified NLSS* such that $\dot{\mathbf{x}} = f_s(\mathbf{x}, \mathbf{u})$, more tractable for its manipulation and derivation of control laws. The cost of these simplifications, such as the consideration of constant thermodynamic properties, is the increase of modelling error. A difference in comparison with Pérez-Roca S. et al. (2018) is the consideration of cavity temperatures as correlated functions of the respective MR , thereby shortening the state vector. Besides, in this paper, all equations, states and control have been rendered non-dimensional with respect to the nominal equilibrium values. In terms of notation, the presence of a tilde ($\tilde{\cdot}$) on top of a quantity means that it is dimensional and its absence means the contrary.

The number of states is $n = 12$ and $m = 5$ is the number of control inputs. Here, the state vector \mathbf{x} , of both NLSS, comprises the two turbopumps speeds ω_H and ω_O , the four pressures in the system (p_{CC} of combustion chamber, p_{GG} of the GG, p_{LTH} for hydrogen-turbine inlet cavity and p_{VGC} for oxygen-turbine inlet cavity) and six mass flows, including the ones streaming through control valves (\dot{m}_{VCH} , \dot{m}_{VCO} , \dot{m}_{VGH} , \dot{m}_{VGO} and \dot{m}_{VGC}) and the one streaming through the hydrogen-turbine inlet pipe \dot{m}_{LTH} .

$$\mathbf{x} = [\omega_H \ \omega_O \ p_{CC} \ p_{GG} \ p_{LTH} \ p_{VGC} \ \dot{m}_{LTH} \ \dot{m}_{VCH} \ \dot{m}_{VCO} \ \dot{m}_{VGH} \ \dot{m}_{VGO} \ \dot{m}_{VGC}]^T. \quad (1)$$

The states with greater tracking relevance are incorporated into a reduced state vector \mathbf{x}_z :

$$\mathbf{x}_z = [p_{CC} \dot{m}_{VCH} \dot{m}_{VCO} \dot{m}_{VGH} \dot{m}_{VGO}]^T. \quad (2)$$

The control input \mathbf{u} contains the sections of the five control valves:

$$\mathbf{u} = [A_{VCH} A_{VCO} A_{VGH} A_{VGO} A_{VGC}]^T. \quad (3)$$

Modelling error is specially present in mass flows, which can present a mismatch of 10 to 25% at each step of simplification (simulator, f_c , f_s and linearised models). Errors in the other states are generally below 10% at each step. The state is assumed to be fully measurable in the real engine. This is a realistic assumption for ω and p . However, measuring some mass flows would be problematic in terms of engine design. Mass flows are generally not measured in LPRE, but estimated through pressure, temperature and volumetric flow measurements. This estimation process is deemed perfect in this paper.

3. CONTROLLER DESIGN

The goal of the controller is to drive the state towards a desired reference \mathbf{x}_r at the end of the start-up transient, with a special focus on having a small tracking error in \mathbf{x}_z . At the same time, a set of hard constraints on \mathbf{x} and \mathbf{u} has to be met throughout the transient. This second goal is somewhat more important than the former in order to avoid excessive temperatures, p or ω during engine's operation. The duration of the start-up transient until reaching the reference is required to range between 2 and 4s, which allows the system to cope with possible perturbations or uncertainties while complying with constraints. A concrete reference trajectory is not imposed.

The designed controller comprises two main parts. The main component is the MPC block, which receives a full-state reference and drives the system to it while satisfying constraints. The other part of the controller consists in a preprocessing block, which serves to generate the full reference vector \mathbf{x}_r fed to the MPC. The whole control diagram is depicted in Fig.2. The remaining elements in that diagram are the following. To the right there is the simulation of the rocket engine (complex simulator), run at $10^{-5}s$ for capturing fast dynamics and for being robust to numerical stiffness. The inputs of that simulator and of the state-space model used for control are valve sections \mathbf{u} . However, the actuators model (internal valve actuators) requires an input in terms of α . That is the reason why there is a conversion block, characterised by static and monotone nonlinear functions. The MPC controller provides valve sections that are then translated into angles. The cause for considering valve actuators as a separate entity is the fact that they represent an internal servo-loop, in which the angular position of the valve is tuned by means of a hydraulic or electrical actuator, modelled as a second-order system.

3.1 Preprocessing

The preprocessing block serves as an off-line reference generator for the MPC controller. This is required because the set of reference commands derived from launcher needs is not sufficient to provide a complete-state target equilibrium point to the engine controller. Hence, a way of restoring a full state vector from those data is necessary. In addition, without this \mathbf{x}_r , the posterior MPC controller

would not attain the tracking goal with high precision. This is mainly due to the fact that f_s is linearised about \mathbf{x}_r , as explained in Section 3.2.

As said before, \mathbf{x} presents twelve states, and there are four reference inputs: $p_{CC,r}$, $MR_{PI,r}$, $MR_{CC,r}$ and $MR_{GG,r}$. Moreover, the last three, in contrast to p_{CC} , do not directly correspond to states in the model. They establish relations between \dot{m}_i . In a first place, thanks to the selected pressure and $MR_{CC,r}$, the choked-flow static equation

$$\dot{m}_{CC} = \frac{p_{CC} A_{th}}{C^*} \quad (4)$$

can provide \dot{m}_{VCH} and \dot{m}_{VCO} , where A_{th} is the throat area and C^* is the characteristic velocity, dependent on MR itself. Then, the rest of states at equilibrium are computed by solving the following overdetermined system of nonlinear equations:

$$\begin{cases} \dot{\mathbf{x}} = f_c(\mathbf{x}_r, \mathbf{u}_r) = 0 & \setminus (\dot{p}_{CC} = 0) \\ \frac{\dot{m}_{VCO} + \dot{m}_{VGO}}{\dot{m}_{VCH} + \dot{m}_{VGH}} = MR_{PI,r} \\ \frac{\dot{m}_{VGO}}{\dot{m}_{VGH}} = MR_{GG,r} \\ \dot{m}_{VGH} + \dot{m}_{VGO} = \dot{m}_{LTH} + \dot{m}_{VGC}. \end{cases} \quad (5)$$

The first equations force the ODE to be at equilibrium, the second and the third ones determine the MR and the last one enforces the equilibrium of $\sum \dot{m}_i$ in the GG. The ODE for \dot{p}_{CC} is removed since it is completely dependent on the reference inputs, not providing additional information. This resolution is performed numerically via nonlinear least squares due to the unavailability of an analytic solution of the system, of either f_c or f_s . The complex model has been chosen to increase accuracy.

3.2 MPC algorithm

MPC predicts the future system behaviour along a horizon, and optimises control inputs according to a cost function generally related to a reference trajectory or to an end state. In this paper, the dynamic model used in the state-feedback MPC controller is considered as a linearisation of f_s about the previously computed $(\mathbf{x}_r, \mathbf{u}_r)$ and as a zero-order hold discretisation at $\Delta t = 10ms$ (due to computational constraints):

$$\Delta \mathbf{x}_{k+1} = A_d(\mathbf{x}_r, \mathbf{u}_r) \Delta \mathbf{x}_k + B_d(\mathbf{x}_r, \mathbf{u}_r) \Delta \mathbf{u}_k \quad (6)$$

Thus, in linear terms, the goal of the controller is to find the set of $\Delta \mathbf{u} = \mathbf{u} - \mathbf{u}_r$ that drives the state to $\Delta \mathbf{x} = \mathbf{x} - \mathbf{x}_r = \mathbf{0}$. The matrix A_d is stable for all the physically feasible \mathbf{x}_r , which is a particularity of GG-cycle LPRE. In this MPC section, in order to lighten notation, all \mathbf{x} and \mathbf{u} refer to variations with respect to the equilibrium point. The approach carried out is partially based on the quasi-infinite horizon (QIH) approach by Chen H. and Allgoewer F. (1998), because it presents proofs for guaranteed stability and end-state reachability of MPC by incorporating the notion of a terminal region. The MPC drives the system to that region, where a fictitious local controller K performs the precise tracking at the end of the state prediction horizon, $N_p + 1$. However, in MPC only the first computed control, $\mathbf{u}_{MPC} \equiv \mathbf{u}_1$, is transmitted to the plant. Hence, the real role of the fictitious feedback $\mathbf{u}_{N_p+1} = K \mathbf{x}_{N_p+1}$ is to compute the P

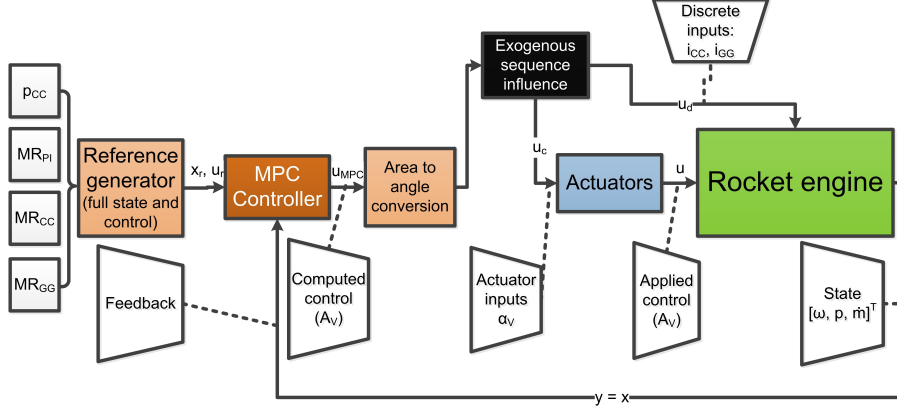


Fig. 2. Control-loop diagram

matrix of a Lyapunov function $V(\mathbf{x}) = \mathbf{x}^T P \mathbf{x}$, by solving the following Lyapunov equation:

$$(A_K + \kappa I)^T P + P(A_K + \kappa I) = -Q_K - K^T R_K K. \quad (7)$$

In (7), the compound of the linear system with a simple LQR feedback controller is considered, $A_K = A_c + B_c K$ (where A_c is the continuous counterpart of A_d), $\kappa \in \mathbb{R}^+$ (satisfying $\kappa < -\lambda_{max}(A_K)$) and Q_K and R_K are positive definite symmetric matrices $Q_K \in \mathbb{R}^{n \times n}$, $R_K \in \mathbb{R}^{m \times m}$. The computed $P \in \mathbb{R}^{n \times n}$ serves to add an additional terminal-region term in the MPC cost. In addition, an integral action is also included to enforce a more precise tracking on \mathbf{x}_z . Those integral decision variables are denoted by \mathbf{z} and present a corresponding weight matrix $S \in \mathbb{R}^{n_z \times n_z}$ in the cost, whose diagonal is $[1, 0.1, 0.1, 0.1, 0.1]$. Thus, the MPC cost J is defined as:

$$J(\mathbf{x}, \mathbf{u}, \mathbf{z}) = \left(\sum_{k=1}^{N_p} \mathbf{x}_k^T Q \mathbf{x}_k + \sum_{k=1}^{N_u} \mathbf{u}_k^T R \mathbf{u}_k + \sum_{k=1}^{N_p} \mathbf{z}_k^T S \mathbf{z}_k \right) \Delta t + \mathbf{x}_{N_p+1}^T P \mathbf{x}_{N_p+1}, \quad (8)$$

which consists in the traditional quadratic cost on states and controls plus the integral and terminal costs, with a prediction horizon $N_p = 10$ steps (0.1s) and a control horizon $N_u = 5$. Implicitly, the last control \mathbf{u}_{N_u} is used for $k \geq N_u$. Further extensions of these horizons did not improve the solutions in terms of tracking or constraints satisfaction. Q and R are positive-definite symmetric weighting matrices $Q \in \mathbb{R}^{n \times n}$, $R \in \mathbb{R}^{m \times m}$, whose diagonals have been computed off-line via Kriging-based black-box optimisation as in Marzat J. et al. (2010). The criterion for that weight selection concerns the minimisation of static error and overshoot in simulations.

Furthermore, the first steps towards a robust consideration of the problem have been implemented. The minimisation of the previous J under constraints is not robust. Indeed, robustness to parameters and initial conditions variations, perturbations and modelling error is very important in this application. Robust MPC approaches generally make use of the *minimax* optimisation, which minimises the worst-case scenario. A generic expression of this problem is the following, in which \mathbf{w} represents disturbance (Mayne D.Q. et al. (2000)):

$$\begin{aligned} \min_{\mathbf{u}} \max_{\mathbf{w}} \quad & J(\mathbf{x}, \mathbf{u}) \\ \text{s.t.} \quad & \mathbf{x} \in X \quad \forall \mathbf{w} \in \mathbb{W}^n \\ & \mathbf{u} \in U \quad \forall \mathbf{w} \in \mathbb{W}^n \end{aligned} \quad (9)$$

However, solving (9) for all possible perturbations is too computationally costly for this application. Hence, it has been opted for choosing a finite set of disturbance scenarios (in a similar manner to Calafiore G.C. and Fagiano L. (2013)) and for solving an equivalent formulation based on Loefberg J. (2003). Concretely, it consists in minimising $\gamma \in \mathbb{R}^+$ via an epigraph formulation. In this paper, that γ constrains the J of the original problem evaluated at several perturbed states propagations \mathbf{x}_i :

$$\begin{aligned} \mathbf{x}_i &= [\mathbf{x}_{i,1}, \dots, \mathbf{x}_{i,k}, \dots, \mathbf{x}_{i,N_p+1}]^T, \quad i \in I \\ \mathbf{x}_{i,k+1} &= A_d \mathbf{x}_{i,k} + B_d \mathbf{u}_k + \mathbf{w}_{i,k}, \quad k \in [0, N_p + 1], \end{aligned} \quad (10)$$

where $\mathbf{w}_{i,k}$ are certain selected perturbation vectors belonging to $\mathbb{W} = \{\mathbf{w}_{i,k}, i \in I, k \in [0, N_p + 1]\}$. I is a finite set, which serves to index the considered perturbation cases. Indeed, the epigraph formulation allows to entirely shift the robustness considerations into the list of constraints. Therefore, only a smooth convex nonlinear programme (NLP) is required, which is more computationally tractable than (9). The minimisation problem proposed here, in which decision variables are extended to consider all \mathbf{x}_i , is described below:

$$\begin{aligned} \min_{\mathbf{x}_i, \mathbf{u}, \mathbf{z}_i, \gamma} \quad & \gamma \\ \text{s.t.} \quad & J(\mathbf{x}_i, \mathbf{u}, \mathbf{z}_i) \leq \gamma \quad \forall i \in I \\ & \mathbf{x}_i \in X, \quad \mathbf{u} \in U \quad \forall i \in I \\ & A_{ineq}[\mathbf{x}_i \quad \mathbf{u}]^T \leq \mathbf{b}_{ineq} \quad \forall i \in I \\ & A_{eq}[\mathbf{x}_i \quad \mathbf{u}]^T = \mathbf{b}_{i,eq} \quad \forall i \in I \\ & \mathbf{x}_{i,N_p+1}^T P \mathbf{x}_{i,N_p+1} \leq \alpha_P \quad \forall i \in I \\ & \mathbf{z}_{i,k+1} = \mathbf{z}_{i,k} + \Delta t K_I \mathbf{x}_{z,i,k} \quad \forall i \in I, k \in [0, N_p]. \end{aligned} \quad (11)$$

X and U are the allowable sets for states and control (compact subsets of $\mathbb{R}^{n(N_p+1)}$ and \mathbb{R}^{mN_u} respectively). The set U for the first control \mathbf{u}_{MPC} is specially constrained to comply with actuators capacity (Luo Y. et al. (2004)):

$\mathbf{u}_{MPC} \in [\max(\underline{U}, \mathbf{u}_0 - \dot{\mathbf{u}}_{max} \Delta t), \min(\overline{U}, \mathbf{u}_0 + \dot{\mathbf{u}}_{max} \Delta t)]$, where \mathbf{u}_0 is the previous-step control (warm start is performed) and $\dot{\mathbf{u}}_{max}$ is the maximum sectional velocity of valves. Regarding the rest of constraints, (11) contains equality constraints (defined by A_{eq} and $\mathbf{b}_{i,eq}$) for linear dynamics (10) and also linear inequality constraints

(defined by A_{ineq} and \mathbf{b}_{ineq}), for complying with MR and actuators sectional-velocity bounds at all \mathbf{x}_i . In relation to the terminal region, a constant α_P refers to the neighbourhood in which the Lyapunov term of J is constrained in a nonlinear way (further details on the QIH method in Chen H. and Allgoewer F. (1998)). The different $\mathbf{w}_{i,k}$ represent the various ways in which the system can evolve after an unknown perturbation or uncertainty in the state, and hence it is proposed to estimate them by analysing the modes of the system (eigenvectors of A_c). The total number of perturbation cases $I = \{1, 2, 3\}$ corresponds to a subset of the eigenvectors. In this manner, the structural information of A_c is used to define unfavourable disturbance scenarios, similarly to Yedavalli R.K. (1985). The modulus of the vectors $\mathbf{w}_{i,k}$ is kept equal to 0.1. It is important to emphasise the fact that the resulting \mathbf{u} obtained in (11) has been confronted to all these perturbation scenarios and that all propagated perturbed states must comply with all constraints, thereby improving the robustness of the controller. This approach with equality constraints within an uncertain problem is only valid because of the finite choice of $\mathbf{w}_{i,k}$. The last line in constraints corresponds to the integrator dynamics (Santos L.O. et al. (2001)), where K_I is a gain matrix computed off-line in the same manner as Q and R .

4. ANALYSIS OF RESULTS

The interior-point optimisation software *IPOPT* (Wachter A. and Biegler L.T. (2006)) has been used to solve this smooth convex NLP within the *MATLAB* environment. Simulations of the previously presented control loop are run from 1.5s until 3s after the start command, that is to say, during the time window in which continuous control is possible in engine start-up transient. Mixture ratios naturally start from values very far from the allowable area, due to the low initial mass flows that hinder the definition of quotients. Indeed, chambers are not physically ignited during the first instants (even if igniters are active); hence, MR are not relevant there. Fig. 3 depicts the results of p_{CC} tracking for three operating points: $p_{CC,r} = 1$ (nominal), $p_{CC,r} = 0.7$ (minimum for this engine) and $p_{CC,r} = 1.2$ (maximum). At all three points, the reference mixture ratios remain the same $MR_{CC,r} = 6$, $MR_{GG,r} = 1$ and $MR_{PI,r} = 5.25$. MR tracking for the nominal case is depicted in Fig. 4.

Tracking is achieved with sufficient accuracy in p_{CC} for

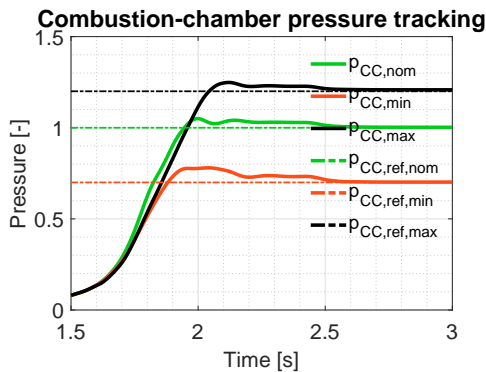


Fig. 3. Tracking results in p_{CC} for $p_{CC,r} = 1$ (nominal), $p_{CC,r} = 0.7$ (minimum) and $p_{CC,r} = 1.2$ (maximum)

all cases (under 0.7%) and with little error in MR (under 0.3% in nominal, under 1.7% in off-nominal) while respecting constraints up from the time when it is considered feasible and acceptable to respect them in practice (1.9s). The overshoot and oscillations present before achieving the final tracking are generated by the exogenous influence of the GG-starter input mass flow, which is not taken into account in the linearised model. Overshoot is more pronounced in the minimum case since the relative influence of the starter is more elevated.

The controller is able to achieve that tracking performance after random initial conditions coming from the sequential transient, whereas constraints-verification time oscillates some hundredths of seconds. Computational times in *MATLAB* are of the order of ten times longer than real time, which does not rule out a future real-machine implementation.

4.1 Comparison with open loop and other linear controllers

Table 1 summarises the comparison between this closed-loop (CL) proposal and OL simulations in terms of some performance indicators. The nominal OL is engine's orig-

Table 1. Performance-indicators comparison between this CL proposal and OL at the three selected operating points

Operating point	Nominal		Minimum		Maximum	
	OL	CL	OL	CL	OL	CL
Settling time (99%) [s]	2.8	2.51	2.67	2.55	2.69	2.53
Overshoot (% in p_{CC})	6.31	5.04	15.1	11.46	3.34	4.04
Constraints verification [s]	1.81	1.8	1.83	1.76	1.77	1.81
p_{CC} static error (%)	0.25	0.26	2.8	0.26	0.34	0.67
MR_{CC} static error (%)	0.17	0.01	2.58	1.38	3.18	1.37
MR_{GG} static error (%)	1.39	0.05	1.31	0.69	1.23	0.59
MR_{PI} static error (%)	1.43	0.3	2.84	0.85	3.41	1.64

inal command, which is precisely tuned for the standard case. The minimum and maximum OL commands have been computed by means of the preprocessor explained in Section 3.1. The improvement with respect to OL is not dramatic, it is even worse in some indicators. Nonetheless, the real gain of this CL MPC control appears for operating points different from the nominal, where multivariable tracking was difficult to achieve with high performance while respecting constraints during the transient.

Moreover, other linear control methods have been tested on the same plant, such as simple PID and LQR controllers. Tracking results of these controllers are good in

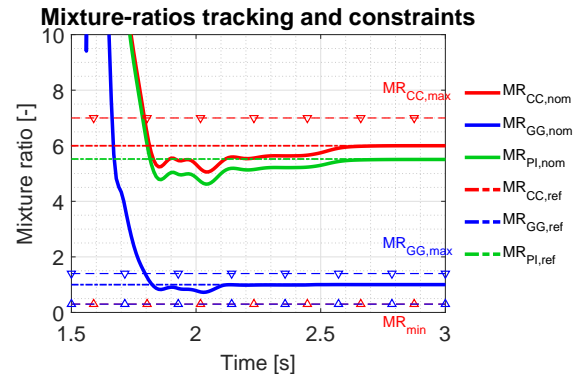


Fig. 4. Tracking results in MR for $p_{CC,r} = 1$ (nominal)

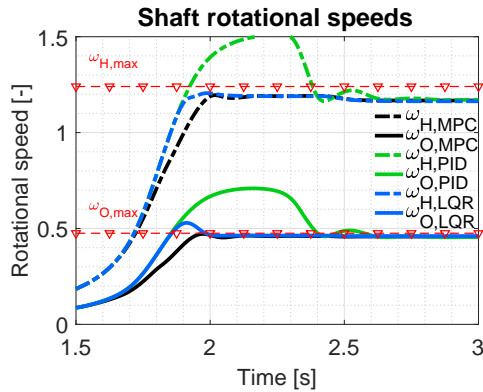


Fig. 5. Rotational speeds ω_H and ω_O for $p_{CC,r} = 1.2$ with MPC, PID and LQR controllers

some of the reference variables (under 0.0001% in p_{CC}), but not for all of them simultaneously. Moreover, there are no guarantees of complying with all the constraints in this problem. Hence, when aiming at tracking off-nominal points, constraints are indeed highly violated. For instance, while throttling up until $p_{CC} = 1.2$, the system controlled by PID or LQR has the tendency to surpass rotational speeds bounds, as depicted in Fig. 5, whereas MPC respects them.

5. CONCLUSION

The control of the transient phases of liquid-propellant rocket engines has traditionally been performed in open loop due to its highly nonlinear behaviour. This work has sought to improve the control of the fully continuous part of the start-up of a gas-generator-cycle LPRE, whose valves can be adjusted for controlling pressure in the main chamber and mass-flow mixture ratios. An MPC controller has been synthesised on that phase for tracking combustion-chamber pressure and mixture ratios while respecting a set of hard operational constraints. This controller is accompanied by a preprocessor that serves to provide a full-state reference built from launcher needs, by making use of a nonlinear state-space model of the engine. The linear MPC controller with integral action is able to track that end-state reference with sufficient accuracy and constraints are respected when necessary. Robustness, vital in this application with possible perturbations and internal-parameter variations, is taken into account for a given set of perturbation scenarios. The costly nested *minimax* optimisation of typical robust MPC approaches has been rewritten as the minimisation of a scalar cost. In future work, other ways of posing this robustness consideration globally will be investigated. The tracking of a predefined trajectory will also be studied. A more extensive validation study with respect to perturbation cases will be carried out.

REFERENCES

Baiocco P. and Bonnal C. (2016). Technology demonstration for reusable launchers. *Acta Astronautica*, 120, 43–58.

Calafiore G.C. and Fagiano L. (2013). Robust Model Predictive Control via Scenario Optimization. *IEEE Transactions on Automatic Control*, 58(1), 219–224.

Chen H. and Allgöwer F. (1998). A Quasi-Infinite Horizon Nonlinear Model Predictive Control Scheme with Guaranteed Stability. *Automatica*, 34(10), 1205–1217.

Dai X. and Ray A. (1996). Damage-Mitigating Control of a Reusable Rocket Engine: Part II-Formulation of an Optimal Policy. *Journal of Dynamic Systems, Measurement, and Control*, 118(3), 409–415.

Loefberg J. (2003). *Minimax Approaches to Robust Model Predictive Control*. Number No. 812 in Linköping Studies in Science and Technology Dissertations. UniTryck.

Lorenzo C.F., Ray A., and Holmes M.S. (2001). Nonlinear control of a reusable rocket engine for life extension. *Journal of Propulsion and Power*, 17(5), 998–1004.

Luo Y., Serrani A., Yurkovich S., Doman D.B., and Oppenheimer M.W. (2004). Model predictive dynamic control allocation with actuator dynamics. In *Proceedings of the 2004 American Control Conference*, volume 2, 1695–1700. Boston, USA.

Marzat J., Walter E., Piet-Lahanier H., and Damongeot F. (2010). Automatic tuning via Kriging-based optimization of methods for fault detection and isolation. In *2010 Conference on Control and Fault-Tolerant Systems (SysTol)*, 505–510. Nice, France.

Mayne D.Q., Rawlings J.B., Rao C.V., and Sckaert P.O.M. (2000). Constrained model predictive control: Stability and optimality. *Automatica*, 36(6), 789–814.

Musgrave J.L., Guo T.H., Wong E., and Duyar A. (1996). Real-time accommodation of actuator faults on a reusable rocket engine. *IEEE transactions on control systems technology*, 5(1), 100–109.

Nemeth E., Anderson R., Ols J., and Olsasky M. (1991). Reusable rocket engine intelligent control system framework design, phase 2. Technical Report NASA Contractor Report 187213, Rockwell International, Canoga Park, California.

Pérez-Roca S., Langlois N., Marzat J., Piet-Lahanier H., Galeotta M., Farago F., and Le Gonidec S. (2018). Derivation and Analysis of a State-Space Model for Transient Control of Liquid-Propellant Rocket Engines. In *2018 9th International Conference on Mechanical and Aerospace Engineering (ICMAE)*, 58–67. Budapest, Hungary.

Pérez-Roca S., Marzat J., Piet-Lahanier H., Langlois N., Farago F., Galeotta M., and Le Gonidec S. (2019). A survey of automatic control methods for liquid-propellant rocket engines. *Progress in Aerospace Sciences*, 107, 63–84.

Santos L.O., Afonso P.A.F.N.A., Castro J.A.A.M., Oliveira N.M.C., and Biegler L.T. (2001). On-line implementation of nonlinear MPC: an experimental case study. *Control Engineering Practice*, 9(8), 847–857.

Saudemont R. and Le Gonidec S. (2000). Study of a robust control law based on H.infinity for the Vulcain rocket engine ArianeGroup internal report, ArianeGroup, ESTACA.

Wächter A. and Biegler L.T. (2006). On the implementation of an interior-point filter line-search algorithm for large-scale nonlinear programming. *Mathematical Programming*, 106(1), 25–57.

Yedavalli R.K. (1985). Improved measures of stability robustness for linear state space models. *IEEE Transactions on Automatic Control*, 30(6), 577–579.